Building and Environment 118 (2017) 313–322

Contents lists available at ScienceDirect

Building and Environment

journal homepage: www.elsevier.com/locate/buildenv

Investigating a selection of mixing times for transient pollutants in mechanically ventilated, isothermal rooms using automated computational fluid dynamics analysis

T.G. Foat [a, b, *], J. Nally [a], S.T. Parker [a]

[a] Dstl, Porton Down, Salisbury, Wiltshire SP4 0JQ, UK
[b] Faculty of Engineering and the Environment, University of Southampton, Hampshire SO17 1BJ, UK

ARTICLE INFO

Article history:
Received 1 September 2016
Received in revised form
11 January 2017
Accepted 11 January 2017
Available online 31 March 2017

Keywords:
Indoor dispersion
CFD
Mixing
Pollutant
Safety
Automation

ABSTRACT

Understanding mixing times for transient pollutants in mechanically ventilated rooms is important for resilience and safety planning for accidental releases of toxic material. There is a lack of information on the ability of simple models available to predict these times for ventilated spaces with different geometries and ventilation configurations. Three analytical mixing time models, including a novel jet transit based approach, have been selected for comparison with computational fluid dynamics (CFD) predictions for a wide range of cuboidal rooms with ceiling ventilation. A modelling tool has been developed, using open source and open source based software, to automatically build and run a large number of Reynolds averaged Navier-Stokes CFD models. The tool has been used to study the dependence of the chosen mixing metrics on room geometry and ventilation parameters, such as the air change rate, for a transient pollutant entering the room via the ventilation system. The room volume, shape, air change rate and vent layout were varied for each room using a Sobol sequence experimental design. The CFD tool has been used to assess the validity of the analytical mixing time models and to derive parameters for the scenarios of interest.

1. Introduction

People within buildings may potentially be exposed to short duration toxic airborne material from a number of different sources, such as an accidental release of a toxic industrial chemical or an intentional release by a terrorist. The source could be outside the building, within the building but in a different room, or within the room where the people are located. For the first two of these scenarios, if the building is mechanically ventilated, the bulk of the material may reach people via transport through the building's heating, ventilation and air conditioning (HVAC) system. In the first case, there may also be a minor contribution via passive infiltration. If a toxic release is detected upon reaching the ventilation intake, then the time available to take remedial action is the sum of the transit time in the HVAC ductwork and the time taken for the material to mix across the room and reach a toxic threshold concentration or exposure at the location of the occupants. HVAC duct transit times may vary from seconds to tens of seconds depending on the length of the ductwork [1]. For an example mechanically ventilated room with an air change rate of 5 h^{-1}, a volume of 184 m^3 and an inlet grille area of 0.15 m^2, Drescher et al. [2] calculated the time for a short duration point source release of a tracer to mix across the room as 444 s. This suggests that the mixing times within the room could be a significant part of the total warning time available. Mixing time here was defined as the time it takes for the concentration distribution (measured at a number of locations in the room) from an instantaneous point source release to achieve a normalised standard deviation of 0.10 or less [3].

Many alternative metrics for the characterisation of mixing in indoor spaces exist and a description of a number of these is given in Refs. [4–6]. Two of the more relevant metrics for assessing the transit of a pollutant across a room are the air change effectiveness and the local mean age of air. The air change effectiveness is the ratio between the shortest time needed to exchange the air in a

* Corresponding author. Dstl, Porton Down, Salisbury, Wiltshire SP4 0JQ, UK.
E-mail address: tgfoat@dstl.gov.uk (T.G. Foat).

http://dx.doi.org/10.1016/j.buildenv.2017.01.011

room (equivalent to room volume divided by total air flow rate) and the mean time. The local mean age of air at a point in the room is defined as the average time taken for air to move from one or more supply inlets to that particular location [7]. While these approaches have many applications, a more relevant measure of mixing, when considering toxic hazards, is the time it takes for different points within a room to reach a concentration threshold.

An understanding of the parameters that govern mixing times in mechanically ventilated rooms will help safety planning and emergency response for releases of toxic material. This type of analysis can be conducted in a number of different ways: analytical, empirical, multizone, zonal and CFD modelling and small-scale or full-scale experiments [8]. Each of these methods has its advantages and disadvantages. For instance analytical models may represent key physical processes but may not apply to complex geometries. Empirical models are rapid but require experimental data to create them. Multizone models do not represent spatial variation in concentration within a zone/room. Zonal models provide some in-zone spatial information but typically do not account for momentum. CFD models can provide high spatial resolution but are currently too slow to run in a responsive mode.

Previously there were no suitable methods to combine the high resolution of CFD with the ability to cover large parameter spaces. One of the aims of this work was to bridge this gap. A tool that could do this could be used in both rapid turnaround emergency response and safety/resilience planning.

In this study, CFD has been used to study the time taken for a transient passive scalar to mix across a range of mechanically ventilated, isothermal, rooms. A tool has been developed to automatically build and run a large number of CFD models in order to study the influence of room geometry and ventilation parameters on selected mixing time metrics. The modelling tool has been developed using open source and open source based software making it possible to simulate many hundreds of cases without incurring prohibitive licence costs. To run and manage the large numbers of cases efficiently, the tool was integrated with the job scheduler on a high performance computing (HPC) cluster. The output from these CFD models has been used to assess the suitability of different analytical mixing time models.

1.1. Mixing time models

The time taken for a pollutant to mix within a room can be estimated using a number of analytical approaches. The most basic mixing model is simply described by the characteristic time of the room, τ [s], which is $1/\lambda$, where λ [s^{-1}] is the room air change rate. Cheng et al. [9] related an eddy diffusion based mixing rate to λ for naturally ventilated residential rooms. Drescher et al. [2] presented a method for calculating mixing in a mechanically ventilated room based on mechanical power input.

This paper presents a study of a selection of previously developed methods (the characteristic time model and the Drescher et al. model) alongside an alternative which focusses on the specific mixing measure of interest in this work. This alternative model is based on the time taken for a jet of contaminated air to move from the supply vent to a plane of interest and for a threshold concentration to be reached at this plane. This model is referred to as the transit time model.

1.1.1. Transit time model

A simplified representation of air flow in an isothermal, mechanically ventilated, room with a ceiling supply diffuser, as described in Cao et al. [10], is shown in Fig. 1, upper. The schematic represents either an entire room or, it is proposed here, a ventilated cell within a room. A ventilated cell is defined as a region in a room containing a single supply vent with its edges located at the point where the wall jets from two adjacent diffusers meet; the vertical dotted line in Fig. 1, lower. The arrows in Fig. 1 illustrate the air jet, containing a pollutant, emanating from a supply diffuser, traveling along the ceiling and then down the wall or the inter-ventilation cell boundary. It is suggested here that the time taken for different points in a room to reach a concentration threshold is governed by the transit of this turbulent jet.

Based on an Equation (1) for normalised velocity decay with distance from an air terminal device for a turbulent wall jet [11], two expressions have been derived for the time taken for the jet to reach a plane by integrating the equation with respect to the distance along the jet.

$$\frac{U_m}{U_0} = \frac{K_v}{\sqrt{x/h_0}}, \tag{1}$$

where U_m [$m \cdot s^{-1}$] is the maximum velocity within the wall jet, U_0 [$m \cdot s^{-1}$] is the average initial velocity, K_v [dimensionless] is the throw constant, x [m] is the distance along the jet and h_0 [m] is the effective height of the diffuser slot. For the equation and constants presented by Awbi [11], h_0 was defined as the square root of the supply duct area. Equation (1) has been extended here to derive a model for the time it takes a jet to transit from the air terminal device to a plane of interest. This model is for the special case where the plane is on the floor, with the assumption that Equation (1) can be used to give velocity for a wall jet turning through 90°. Equation (2) is for the case where the ventilation cell is simplified to a cube and Equation (3) for the non-cube case. The full derivation of the equations is given in the Supplementary Information.

$$t_{transitCube} = C_1 \frac{A_v^{3/4}}{\lambda \sqrt{V_c}}, \tag{2}$$

$$t_{transitAR} = C_2 \frac{\gamma^{3/2} A_v^{3/4}}{\lambda \sqrt{V_c}}, \tag{3}$$

where C_1 [dimensionless] is a constant defined by $\frac{\sqrt{3/2}}{K_v}$. For a square four-way ceiling diffuser, $K_v = 1.93$ [12] and therefore $C_1 = 0.63$. A_v [m^2] is the area of the ceiling diffuser, V_c [m^3] is the volume of the ventilation cell (or the room, if the room only contains one supply diffuser). The constant C_2 [dimensionless] is defined as $\frac{2}{3K_v}$ and $C_2 = 0.35$ for $K_v = 1.93$. γ [dimensionless] is a room geometry factor, given by:

$$\gamma = \frac{1}{2\sqrt[3]{AR}} + AR^{2/3} \tag{4}$$

where AR [dimensionless] is the ventilation cell aspect ratio (H/W_c), W_c [m] is the width of the ventilation cell and H [m] is the height of the room.

Although not explored here, the transit time metric could be related to the local mean age of air. The transit time differs from the local mean age of air in that it includes a concentration threshold (described in Section 2.3) so depends on the chosen threshold relative to the pollutant concentration in the supplied air, as well as the air movement and mixing within the room.

1.1.2. Mechanical power model

Drescher et al. [2] presented a model for mixing time, t_{mix} [s], based on work by Corrsin [13]. The mixing time, t_{mix}, is defined by Baughman et al. [3] as the time for the concentration distribution across a room from a point source release to have a normalised standard deviation, σ_t, of 0.10 or less. Drescher et al. [2] derived the

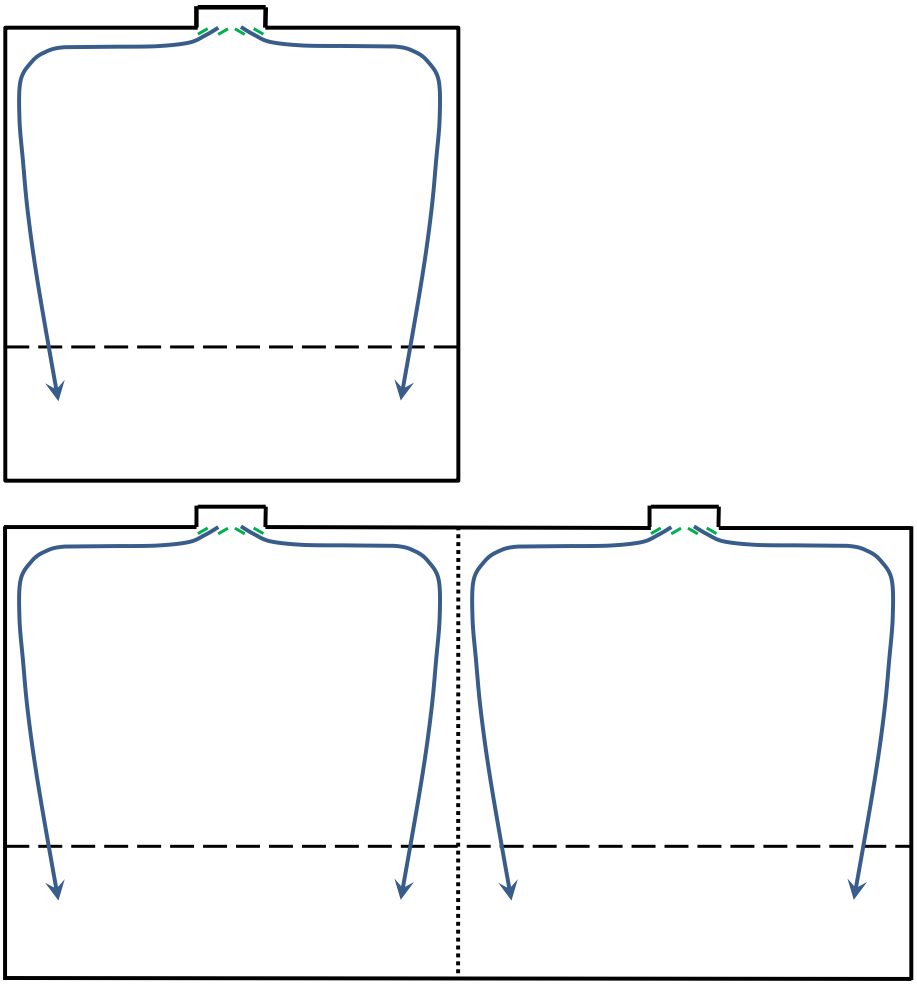

Fig. 1. Schematic of the air flow in a room with a ceiling diffuser containing louvres, representing either an entire room (upper) or ventilated cells within a room (lower). The vertical dotted line indicates the boundary between two adjacent ventilated cells. The plane of interest is shown as a dashed line.

following expression.

$$t_{mix} = C_3 \frac{M^{1/3} L^{2/3}}{P^{1/3}}, \tag{5}$$

where M [kg] is the mass of air in the room, L [m] is the characteristic dimension of the room (assumed by Drescher et al. to be the cube root of the room volume) and P [W] is the mechanical power input. C_3 [dimensionless] was measured to be 17.6 [2] based on experiments in a 31 m^3 room where 0.2 $h^{-1} \leq \lambda \leq 2\ h^{-1}$ with a 20 s duration release of a tracer at a point. Mixing was provided by air movers located in the room without any air extraction/supply. The power, P, was calculated by Drescher et al. using the following expression,

$$P = \rho/2 \sum_{all\ blowers} \left(\int_A U^3 dA \right), \tag{6}$$

where ρ [$kg \cdot m^{-3}$] is the density of the air, U [$m \cdot s^{-1}$] is the velocity in the air blower duct, and A is the cross sectional area of the duct. In their worked example Drescher et al.used the supply air grille dimension, A_v, to arrive at A and the grille discharge air velocity for U. A new equation for t_{mix} can be produced from the Drescher model, relating t_{mix} to A_v, λ and the volume V [m^3]:

$$t_{mix} = C_4 \frac{{A_v}^{2/3}}{\lambda V^{4/9}}. \tag{7}$$

For this equation, V is either the room volume, with A_v being the total vent area in the room (in which case t_{mix} is referred to as $t_{mixRoom}$), or V is the ventilation cell volume, with A_v being equal to the vent area per ventilation cell (in which case t_{mix} is referred to as $t_{mixCell}$). The constant $C_4 = 2^{1/3} C_3$, therefore when $C_3 = 17.6$, $C_4 = 22.2$.

Although this model was developed for a point release of a pollutant within a room, its suitability to represent a release via the ventilation system has been tested here.

Both of the above models assume a turbulent flow and so may not be valid if regions in the room contain laminar air flow or if the wall jet is laminar. Li and Nielsen [14] discussed how a high air change rate (>5 h^{-1}) may be required to produce fully-developed turbulence in isothermal rooms. However, others drivers of air movement in a room, such as natural convection, people movement or mechanical devices [15] could increase the turbulence.

1.1.3. Characteristic time model

For a room with mixing ventilation it might be expected that the time taken for a pollutant concentration to homogenise in a room would depend on the rate at which the air is replaced by supply air.

The characteristic time, τ [s], may therefore be expected to be related to mixing time.

The definitions of t_{mix}, $t_{transit}$ and τ are not the same but are all related to mixing across the space.

2. Methodology

To test the suitability of the three mixing time models described above to represent mixing of a transient, neutrally-buoyant pollutant entering a room via its ventilation system, a novel method to build, setup, run and post process a large number of CFD models has been developed. The method has been used to simulate a range of cases using an experimental design process.

2.1. The automation process

The entire CFD process was automated, from defining and selecting the parameters that describe the specific scenario to be modelled, through to post processing of the results.

A schematic diagram of the automated process is shown in Fig. 2. This automation was implemented using custom Python™ (V2.7.8) code which incorporated interfaces to existing software.

Individual simulations were generated based on a Sobol sequence [16] experimental design created using the R statistical programming language (V2.15). The Sobol sequence is a space filling algorithm which populates the n-dimensional parameter space by selecting the next point from the most sparsely populated region. In this way, the entire range of each parameter shown in Table 1 was covered effectively. Future developments could include a more intelligent method such as a treed Gaussian process [17] to optimise input parameters. This method locates the next experiment based on the results of the previous experiments. Salome V6.5.0 (Open Cascade, France), an open source integration platform for numerical simulation, was used to generate the STL surfaces of the room geometries. IconCFD V3.1.6 (Icon, United Kingdom) was used for the meshing (iconHexMesh [18]) and the CFD solutions (iconSimpleFoam and iconSpeciesFoam [18]).

To ensure the quality of the model output, both the residuals of the steady state simulations and concentration versus time plots for each simulation were checked manually. The models were all built using a validated method as in Section 2.5.

2.2. Modelled scenario

The modelled scenario represents a short duration release of a toxic gaseous pollutant into the ventilation system supplying a room. The pollutant was modelled as a neutrally buoyant passive scalar. Hazardous materials could also be present in the form of an aerosol but this type of material is not considered explicitly here. The transport of an aerosol may differ from that of a gas due to, for example, the inertia of the particles, gravitational settling and deposition onto surfaces. However, if the particles are small, the transport of the gas would be expected to be representative of aerosol transport over short time scales. At longer times, the effect of the increased aerosol decay rate (compared to that of the passive scalar) could result in different mixing times.

Table 1
Experimental design space.

Parameters	Symbol	Ranges
Room volume	V	50 m^3 – 5000 m^3
Floor aspect ratio	L/W	1 – 3
Height/(floor area)$^{1/2}$	H/(L W)$^{1/2}$	0.1 – 1.5
Air change rate	λ	0.5 h^{-1} – 20 h^{-1}
HVAC grille sizes		2 sizes, (0.4 m)^2 or (0.6 m)^2

The rooms were cuboid in shape and contained no furniture. They were served by mixing ventilation with, no recirculation, via supply and extract vents (square four-way diffuser) located in the ceiling. The room volume and shape, the air change rate and vent layout were varied across the parameter space shown in Table 1.

Room geometries were defined using a simple algorithm described below. Supply grilles were based approximately on Trox ADT 4-way discharge grilles [19]. A 0.4 m by 0.4 m grille, designed for a flow rate of 0.115 $m^3 \cdot s^{-1}$, was chosen for rooms with a total flow rate up to 1.15 $m^3 \cdot s^{-1}$, to limit the number of small grilles in the room to ten. A 0.6 m by 0.6 m grille, designed for a flow rate of 0.29 $m^3 \cdot s^{-1}$ was used for higher flow rates. The throw for the 0.4 m grille was quoted as 1.2 m and as 2.1 m for the larger grille [19]. The actual throw will depend on the flow rate through the grill but to keep the automation process simple, this value was fixed. The number of supply vents in the room was initially calculated based on the throw and guidance given in Awbi [11] which states that "the throw should ideally be equal to the distance from a wall or half the distance to the next adjacent diffuser". This method for calculating the number of vents gave what appeared to be an excessive number of vents so the throw value was multiplied by an arbitrary factor of 1.5, reducing the number of vents by $1/\sqrt{1.5}$. The angle of the louvres on the supply grille was set to 30° to the horizontal. The extract grilles were based approximately on Trox Eggcrate Grille Type AE [19]. Two sizes of grille were used: 0.4 m by 0.4 m and 0.6 m by 0.6 m. The smallest grilles were used for total room flow rates less than 5.0 $m^3 \cdot s^{-1}$ and the largest grilles for higher flow rates. The number of vents was chosen so that the mean velocity through the grille was approximately 4 $m \cdot s^{-1}$ [12], this limited the number of small grilles in the room to eight.

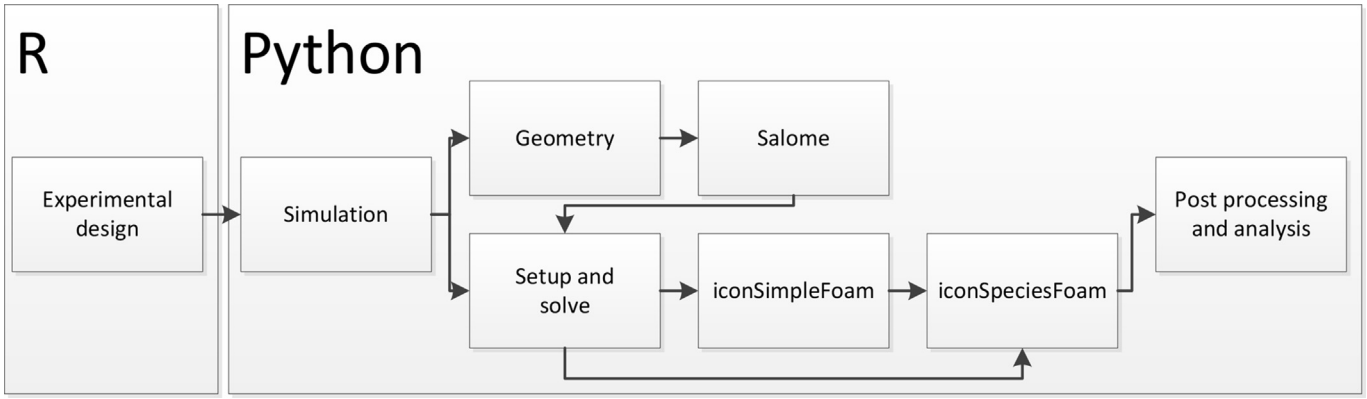

Fig. 2. Diagrammatic representation of the automated process.

Supply and extract vents were distributed across the ceiling in rows with a row of extracts between rows of supplies. The total number of supply and extract rows was determined based on the width of the room. The rows were uniformly spaced across the room and vents were uniformly spaces in each row. Cases were not considered if the ratio of number of extracts to number of supplies was less than 0.1. Six example room plan views are shown in Fig. 3.

The room height was limited to a minimum of 2.5 m, taken as a lower bound for standard rooms. The floor aspect ratio and height/(floor area)$^{1/2}$ were chosen to represent a broad but realistic range or rooms. The smallest room volume, 50 m^3, could represent a small hotel room or meeting room. The largest volume was set to 5000 m^3 as it was felt that rooms larger than this are more likely to be of a more bespoke design and would not have standard ceiling mounted mixing ventilation. The minimum and maximum air change rates were set to 0.5 h^{-1} and 20 h^{-1} to cover a broad range of total air change rates for occupied spaces.

A time delay was included to account for the time of travel from the release location in the HVAC ductwork to each supply diffuser. It was assumed that the pollutant was delivered into the HVAC ductwork at one end of the room. The delay was calculated based on the distance from the end of the room (along the longest axis only) to the middle of each vent and it was assumed that the air was moving at 2.75 m·s^{-1}, based on the average of values for HVAC branch supply ducts from Porges [20]. The upper recommended value for main supply ducts is 8 m·s^{-1} so it is possible that the delay time could be shorter than those chosen for this study. If the release took place in the HVAC plant room, there would be an additional delay time due to the transit from the release point to the ductwork above the room. More detailed models for pollutant transport in HVAC ductwork exist, e.g. Ref. [21], and these could be used to provide a more resolved input concentration profile.

Pollutant concentrations were calculated by the model for three horizontal planes with heights, 0.5 m, 1.0 m and 1.5 m. These planes were chosen to cover the occupied zone.

Approximately 100 CFD models were run per analysis and these could easily be run within a few days on a reasonable size HPC cluster.

2.3. Pollutant release mass

In order to make the study as generic as possible, the toxic threshold, $C_{threshold}$ [kg·m^{-3}], was calculated as a function of the release mass, M [kg]. The release mass was calculated for each geometry so that in a well-mixed room of the defined size and flow rate, a specified peak concentration (in time), C_{peak} [kg·m^{-3}] would be reached.

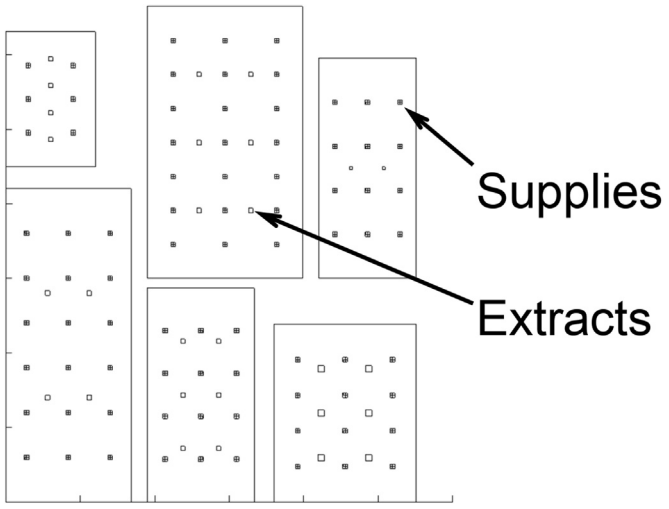

Fig. 3. Plan views of six example rooms showing the supply and extract vent layouts. The supply vents are shaded, the extracts are open squares. The tick marks on the axes are spaced at 10 m intervals.

The concentration of a gaseous pollutant, released at a constant rate, S [kg·s^{-1}], into a room, assuming the room can be represented by a well-mixed zone, is given by the following according to, for example, Keil et al. [22].

$$C = \frac{S}{Q}\left[1 - e^{(-\lambda \cdot t)}\right], \tag{8}$$

where Q [m^3·s^{-1}] is the volume flow rate into and out of the room and t [s] is the time from the start of the release. If the release has a finite duration, then the peak concentration is reached when $t = \Delta t$, where Δt [s] is the duration of the release. For a finite duration release, the release mass, M, is given by $S \cdot \Delta t$. Therefore the release mass required to achieve a specified peak concentration, C_{peak}, in a well-mixed space is given by the following:

$$M = \frac{C_{peak}\, Q}{\left[1 - e^{(-\lambda \cdot \Delta t)}\right]}\Delta t \tag{9}$$

For this study, Δt was set to 1 s, 10 s or 100 s.

The peak concentration, C_{peak}, was defined as a function of a threshold concentration, with $C_{peak}/C_{threshold}$ equal to either 10 or 100.

2.4. Mixing metrics

Three different mixing time metrics were calculated from the CFD scalar concentration data, across the three planes, to compare to the mixing time models described in Section 1.1. The first was the time taken for the normalised standard deviation of concentration to reduce to 0.10, t_σ [s] [3]. The second was equal to the time taken for different proportions of a room to reach a given concentration threshold. If the range of concentrations within the room is described by a distribution, then a useful measure of mixing is given by the difference between the time when only the highest concentrations (the 95th percentile value) cross a threshold ($C_{threshold}$), t_{95} [s], and when all but the lowest do (the 5th percentile value), t_5 [s]. This time is referred to here as $t_{95\text{-}5}$ [s] and is indicative of the time between the first people and the last people in a room being exposed to $C_{threshold}$. A third metric was calculated, to directly compare to the transit time model. This was the time taken for the 95th percentile of concentration across the planes to cross the concentration threshold and is represented by t_{95} [s]. This may be expected to represent the time for material to reach the occupied zone from the supplies.

In order to avoid bias due to any differences in mesh density on the three planes the following procedure was followed. First the percentiles were calculated for each plane separately, then the 95th percentile time was taken as the shortest 95th percentile time across all the planes and the 5th percentile, the longest time.

2.5. The CFD modelling method and method validation

CFD modelling was performed using the software IconCFD V3.1.6. The software and methodology were validated against an indoor dispersion tracer experiment. The validated methodology was then applied in the automated study. The room used for the validation experiment is shown in Fig. 4. The room was 13.0 m long, 7.0 m wide and 2.6 m high with a small cut out in one corner. The room volume was 237 m^3, the floor aspect ratio 1.9 and H/(floor

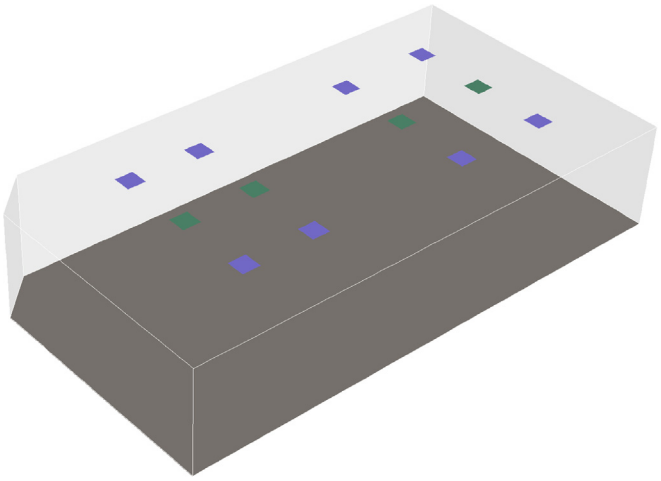

Fig. 4. CFD geometry of the indoor dispersion test case room. The supply vents are coloured blue and the extracts green. (For interpretation of the references to colour in this figure legend, the reader is referred to the web version of this article.)

area)$^{1/2}$ = 0.27. The room had mixing ventilation with the air supplied through eight diffusers and extracted through four. All ceiling diffusers were square, four-way diffusers (0.45 m × 0.45 m). In the experiment, the total air flow rate was 1.0 $m^3 \cdot s^{-1}$ and the recirculation fraction was 0.56, giving a fresh air change rate of 6.8 h^{-1} and total air change rate, λ, of 15.4 h^{-1}. It is worth noting that the HVAC for the automatically generated rooms had no recirculation and this may have a significant effect on mixing, particularly at longer times. For the trial, 40 L of the tracer gas propylene was released over a period of 180 s, just upstream of the HVAC air handling unit and its concentration was monitored in the test room using nine ultra-violet ion collector (UVIC®) Mk II photo-ionisation detectors [23]. Eight of the UVICs were 0.65 m above the ground with one at 1.95 m height. Data from two replicate experiments were used for the CFD validation.

The IconCFD mesher (iconHexMesh) uses cut cell meshing. The starting base mesh was 0.25 m with the mesh on the supply and extract vents refined to the 4th and 3rd levels respectively. Cuboid refinement regions were also applied around the supply and extract vents with refinement to the 2nd level. The representation of the geometry was reasonably coarse to enable shorter run times (the results of a mesh dependency study are discussed below). The CFD model was run using the k-ω SST turbulence model which gave good performance against the validation case and was also stable for the range of conditions in the automated study; wall functions were also used. It was assumed that the flow was steady state so the flow field was solved for 2000 iterations then fixed and the species transport solved with 1 s time steps (mean Courant, Friedrichs, Lewy (CFL) number ~ 4). The turbulent Schmidt number, Sc_t, was set to 0.7 (Sc_t number dependence is consider below). Default values (based on Icon best practice) were used for all solver settings and these settings were taken forward to the automated study.

Snapshots of the tracer concentration over four planes are shown in Fig. 5. These show the complexity of the flow and how it may deviate from the simple description shown in Fig. 1 and assumed for the transit time model.

For the validation, minimum, average and maximum tracer concentrations, at the nine UVICs and equivalent locations in the model were compared (Fig. 6). This type of comparison does not directly compare the concentration at one location in the CFD model with one location in the experiment but represents a spatially averaged comparison. The model accurately predicted the

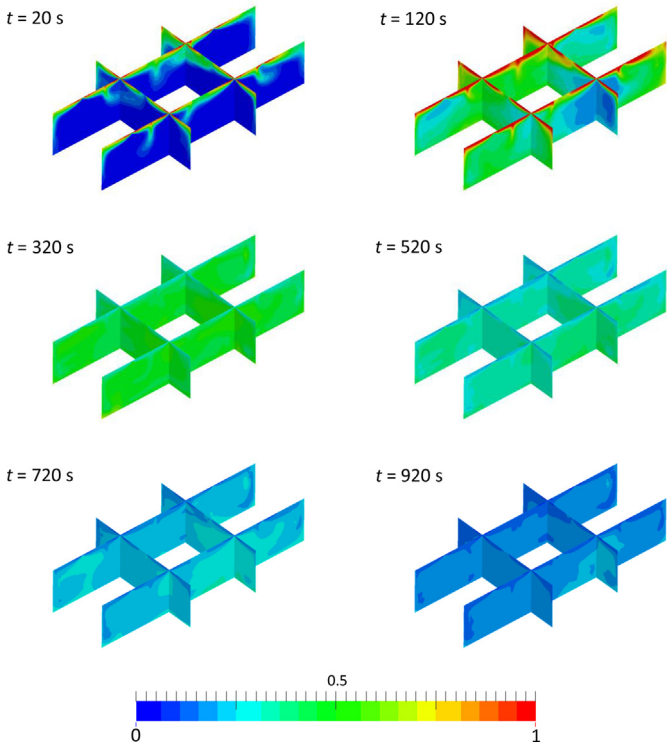

Fig. 5. Contours of tracer mass fraction, normalised to the source concentration at the inlet, on planes passing through the centres of the supplies and some of the extract diffusers. The time after the start of the release is shown next to each image.

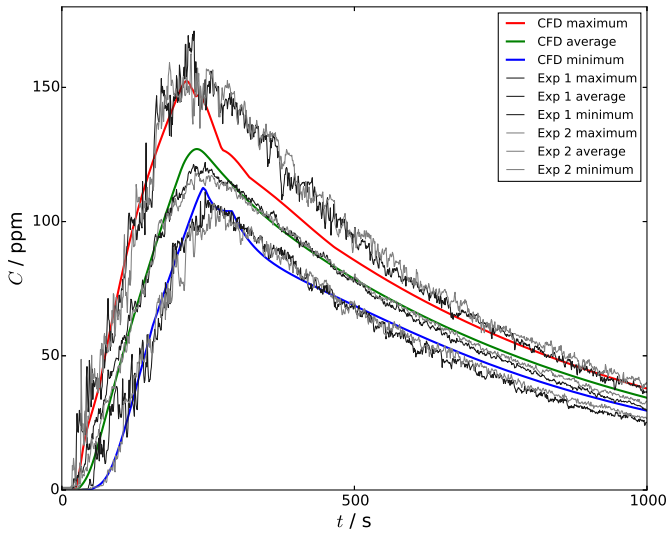

Fig. 6. Maximum, average and minimum tracer concentrations in parts per million (ppm) across nine measurement locations from two experiments compared to predictions from the CFD model.

minimum, average and maximum peaks and the slope of the concentration rise. If the minimum and maximum curves could be considered analogous to the 95th and 5th percentile curves respectively then an accurate prediction of the slope of the concentration rise should result in an accurate prediction of the time it takes the percentiles to cross a threshold concentration, i.e. t_{95} or $t_{95\text{-}5}$. The model slightly under predicted the decay rate as indicated by the difference in the gradients of the experimental and CFD curves. There is also a difference in the concentration range

between the maximum and minimum experimental curves and the maximum and minimum CFD curves. This suggests that the model over predicted the mixing in the decay phase and the result of this would be a small under-prediction of t_σ. The over prediction of the mixing is believed to be caused by the way the ceiling diffusers are simplified in the model. This results in the air jets from the diffusers penetrating too far into the room. The same effect may also be the cause of the under-prediction of the maximum concentration in the period just after the end of the tracer release.

2.5.1. Mesh, time step and turbulent Schmidt number dependency

Mesh dependency was tested by using the validation case with the original base mesh size (0.25 m) increased by a factor of $2^{1/3}$ or reduced by one, two or three factors of $2^{1/3}$, with the time step size altered to maintain the same or a smaller CFL number. The size of the original base mesh (even when applied to the smallest automatically generated room) is at the limits for coarse CFD as defined by Wang and Zhai [24]. The metric t_σ was calculated for each mesh but using only the nine monitor points, rather than a plane as used in the automated study. For the mesh dependency study, the normalised standard deviation target was set to 0.15 as opposed to the 0.10 used in the automated study because the validation room did not reach a normalised standard deviation of 0.10 in all cases. A $t_{95\text{-}5}$ type metric was calculated using the maximum and minimum data, across the nine monitor points, in place of the 95th and 5th percentile series. The results of the mesh dependency study are shown in Fig. 7.

It is clear that the results do have some dependence on mesh size, as is typically the case for indoor air flow CFD [24,25].

Time step size independence was demonstrated by reducing the time step from 1.0 s to 0.5 s (mean CFL changing from approximately 4 to 2) with no significant effect on the result. The dependence of the mixing metrics on the Sc_t was assessed by changing it over a typically applied range of values (0.2–1.3 [26]). For $Sc_t = 0.5$ or 1.3, $t_{95\text{-}5}$ and t_σ varied by ± 3% or less when compared to $Sc_t = 0.7$. Changing Sc_t to 0.2 had a more significant effect with t_σ reducing by 24%.

Using the methods presented here, the results do show some dependence on mesh size and Sc_t. It is felt that this level of dependence is acceptable because of the good agreement with the validation case but the indicative uncertainty ranges given above should be applied to the final modelling output.

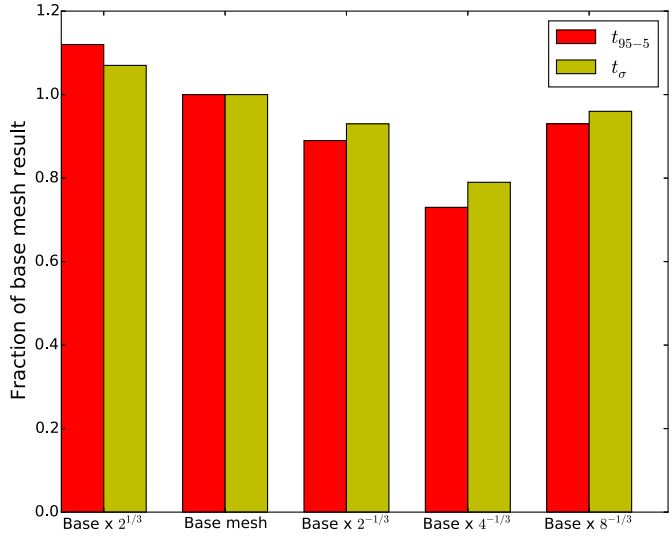

Fig. 7. Results of the mesh dependency study. The coarsest mesh is on the left and the finest on the right.

2.5.2. Buoyancy

It is known that buoyancy can affect indoor air flows and, in particular situations, can cause stratification to occur. The relative importance of buoyancy can be estimated by the ratio of the Grashof number, *Gr*, to the square of the Reynolds number, *Re*. This ratio, the Richardson number, *Ri*, describes the relative importance of natural and forced convection. $Ri > 1$ suggests that buoyancy is important and $Ri < 1$, that forced convection dominates. With mean velocities in mechanically ventilated spaces typically less than 0.2 $m \cdot s^{-1}$ [27] and ventilation cell sizes of the order of 3 m, even a small temperature difference across this space (5 °C) could result in $Ri > 10$ which suggests that buoyancy will affect the flow.

To simplify this initial study the rooms considered were empty of people and other heat sources and buoyancy effects could therefore be ignored.

The presence of buoyancy would be expected to increase the rate of mixing in a room. According to Drivas et al. [28] an increase in temperature difference between the floor and the ceiling of a room will result in a linear increase in the effective diffusivity. Buoyancy sources can also lead to stratification in some cases which reduces the large scale mixing and should be considered in future work.

3. Results

Data for the three metrics described in the methodology (t_σ, $t_{95\text{-}5}$ and t_{95}) were extracted for each automated CFD run and are presented and discussed below. The CFD models were for a short duration release of a gaseous pollutant into the ventilation system of a mechanically ventilated room, as described in Section 2.3. The three metrics are compared to each other in Fig. 8. In some cases t_σ, for a standard deviation of 0.10, was not reached during the total simulation time (1000 s) but the corresponding values of $t_{95\text{-}5}$ are shown on the axes. Figs. 8–11 show data for $\Delta t = 10$ s and $C_{peak}/C_{threshold} = 10$ and in all these figures, each data point represents the output from an individual CFD run.

Fig. 8 shows that t_σ is always longer than $t_{95\text{-}5}$, typically by less than an order of magnitude. In other words the time for the concentration distribution to narrow is longer than the time between the highest concentrations (the 95th percentile value) and the lowest concentrations (5th percentile value) reaching the threshold concentration. The difference between t_σ and t_{95} is greater still, with t_σ more than ten times larger than the time taken for the highest concentrations in the room to reach the threshold. This indicates that the time for a pollutant to reach the sample planes, t_{95}, is shorter than this mixing time, t_σ. Although not plotted here, the times for t_5 are closer to t_σ than t_{95} is. Measures based on other percentiles were not considered in this study but lower percentiles may be closer still to t_σ. However, it should be noted that the t_{95} and t_5 metrics indicate a transport time whereas t_σ indicates when a room becomes mixed so they may never be closely correlated. The right hand plot shows that it takes less time for a pollutant to reach the planes than it does for the material to disperse across the planes.

In order to assess the suitability of the Drescher et al. [2] model to represent mixing of a pollutant which enters a room via the ventilation system, where the room has ceiling supply and extract, t_σ is plotted against the mixing times, $t_{mixRoom}$ and $t_{mixCell}$, calculated using Equation (7), in Fig. 9. The figure also shows $y = x$ as a dotted line. If the data from the Drescher et al. experiment were plotted on this graph, it would be scattered around this line.

A linear regression has been calculated for t_σ and the $t_{mixRoom}$ or $t_{mixCell}$ models, assuming a zero intercept. The correlations with

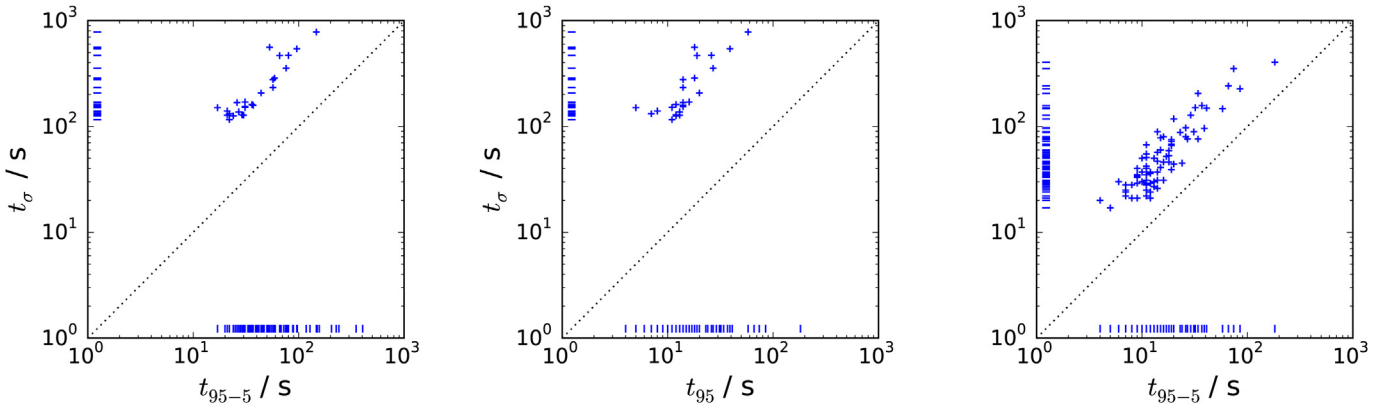

Fig. 8. Three measures of mixing, t_σ, $t_{95\text{-}5}$ and t_{95} plotted against each other on a log-log scale. The line y = x is shown as a dotted line. Values are shown as ticks on the axes to indicate the distribution of values.

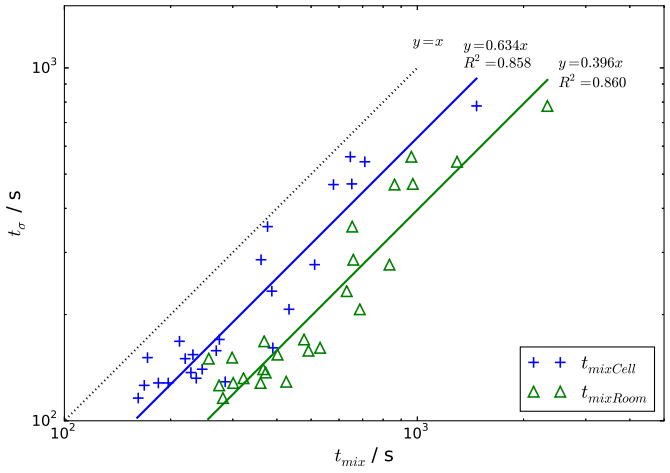

Fig. 9. t_σ plotted against $t_{mixRoom}$ and $t_{mixCell}$ on a log-log scale. The blue and green lines are linear fits with the gradients of the lines and the R^2 values given. The dotted line shows a 1:1 gradient. (For interpretation of the references to colour in this figure legend, the reader is referred to the web version of this article.)

$t_{mixRoom}$ or $t_{mixCell}$ are similar, with R^2 = 0.860 and 0.858 respectively, but with different gradients. The gradient of the $t_{mixCell}$ data is closer to the 1:1 gradient, suggesting that the per cell representation of mixing is closer to the original experiment of Drescher et al. [2] than the whole room representation. The constant calculated by Drescher et al., adjusted to the formulation used in this paper (Equation (7)), C_4, has a value of 22.2. Based on the regression lines, this constant has a value of 8.8 and 14.1 for room and cell models respectively.

It should be noted that only just over 30% of the models run reached the normalised standard deviation threshold of 0.10 in 1000 s. In the remainder of the models, the pollutant was extracted before the threshold was reached. No single variable was found to control whether the threshold was crossed or not.

To reveal the effectiveness of the transit time model at predicting the arrival of a pollutant at the planes of interest, t_{95} is plotted against transit time, $t_{transitCube}$ and $t_{transitAR}$, calculated using Equations (2) and (3), in Fig. 10.

Fig. 10 shows that the transit time model for ventilation cells with defined aspect ratios is a better fit (higher R^2) to the CFD data than the transit time model when the ventilation cell is simplified to a cube. The gradients of the linear fit to the CFD data for both models are very similar. The t_{95} values from the CFD are larger than $t_{transit}$ for the cube and aspect ratio model in most cases, despite the $t_{transit}$ model assuming that the measurement plane is on the floor.

Based on the data shown in Fig. 10, the constant, C_1 in Equation (2), should be changed to 1.23, when the room or ventilation cell is simplified to a cube. C_2 in Equation (3) should be changed to 0.67 when the room is defined in terms of ventilation cells with defined aspect ratios.

Fig. 11 plots $t_{95\text{-}5}$ values from the CFD against the results of three different models, $t_{transitAR}$, $t_{mixCell}$ and τ. Fig. 11 shows a similar R^2 value for a linear regression, when the $t_{95\text{-}5}$ data is plotted against each set of model data, with a slightly higher correlation for τ. This shows that the mixing model of Drescher et al. [2] and the transit time model, Equation (3), are similarly effective in predicting the speed with which material, entering a room via the ventilation system, is transported across the space. The simpler model, based on the air change rate alone is, however, equally effective. Therefore the time between the first people and last people in a room being exposed to a concentration (for which $C_{peak}/C_{threshold}$ = 10 and Δt = 10 s) can be given by the following expression:

$$t_{95-5} = 0.121\,\tau. \tag{10}$$

When $t_{95\text{-}5}$ is plotted against τ for Δt = 1 s, 10 s or 100 s, the gradient of the regression line does not change significantly (0.121 for Δt = 1 s to 0.137 for Δt = 100 s). For $\lambda = 0.5\ h^{-1}$, $t_{95\text{-}5}$ ranges from 871 s to 986 s depending on the release duration and for $\lambda = 20\ h^{-1}$, $t_{95\text{-}5}$ ranges from 22 s to 25 s. The gradient of the regression line exhibits a stronger dependence on $C_{peak}/C_{threshold}$. As $C_{peak}/C_{threshold}$ was increased from 10 to 100, the gradient reduced from 0.121 to 0.097. This indicates that a new set of simulations may be required if $t_{95\text{-}5}$ for larger or smaller values of $C_{peak}/C_{threshold}$ was of interest.

The same data gives relationships between t_{95} and t_5 and τ which may be useful for some applications and are included here for completeness:

$$t_{95} = 0.0389\,\tau \tag{11}$$

$$t_5 = 0.149\,\tau \tag{12}$$

These hold for Δt = 10 s and $C_{peak}/C_{threshold}$ = 10 and have R^2 = 0.917 and 0.967 respectively.

4. Discussion

It has been demonstrated that the Drescher et al. [2] mixing model based on mechanical power can broadly be used to predict the time taken to reach a normalised standard deviation threshold in a mechanically ventilated room with ceiling mounted supply and

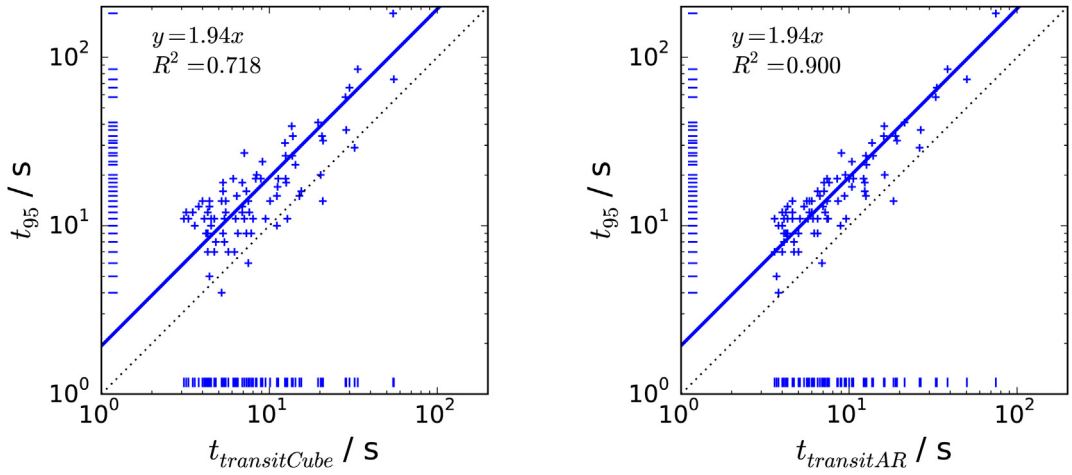

Fig. 10. t_{95} CFD data plotted against the $t_{transitCube}$ and $t_{transitAR}$ model. The solid lines are linear regressions with the gradient of the line and the R^2 value given. The dotted line shows a 1:1 gradient.

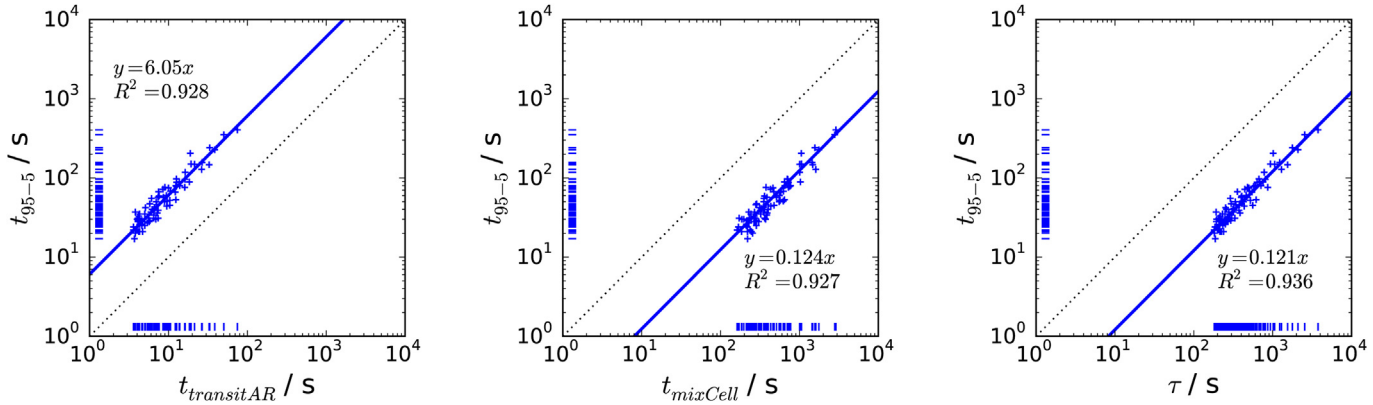

Fig. 11. $t_{95\text{-}5}$ plotted against $t_{transitAR}$, $t_{mixCell}$ and τ. The solid lines are linear regressions with the gradients of the lines and the R^2 values given. The dotted line shows a 1:1 gradient.

extract vents and with the mixed pollutant being delivered via the supplies. The constant required for Equation (7) is smaller than the figure used by Drescher suggesting that, as long as the species is not extracted faster than it can mix, the mixing happens more rapidly in the type of scenario modelled here, compared to that studied by Drescher.

The transit time models developed here explain the majority of the variation observed in the predicted CFD transit time, t_{95}, but in most cases they under predict the time. This may suggest that the flow pattern is not always as simple as that shown in Fig. 1, a point supported by Fig. 4. Jets from the supply vent attach to the ceiling and generally attach to the wall, but when two jets converge from adjacent ventilation cells they follow a more irregular pattern. This irregular pattern may be the cause of the longer transit times. Broadly, the data points nearer to the 1:1 line in Fig. 10 are for rooms with smaller volumes and the further points are for rooms with larger volumes. Smaller rooms typically have fewer inter-ventilation jet convergence regions and relatively more wall jets than the larger rooms.

The Drescher et al. [2] mixing time model, the transit time model and the characteristic time model are similarly effective at predicting the mixing metric $t_{95\text{-}5}$. The analysis conducted here has shown that, for the basic room type studied, a small number of people in the room could experience the threshold concentration in as little as a few seconds after the airborne material enters the room. It could take between an additional 15 s to almost seven minutes for the majority of the people in the room to experience the threshold concentration. The strongest influence of this is the characteristic time, τ. This suggests that for a room with a high air change rate there will be little useful time to evacuate all occupants of a room before they are exposed.

The CFD models used in this study are representative of simplified spaces. For example, they do not contain furniture, heat sources or people. The results cannot safely be extrapolated to more complex spaces which have different supply and extract vent layouts or, perhaps more significantly, regions within the room that are less well ventilated than the main space. Movement of people in the space would be expected to reduce mixing times. The people may also act as heat sources and drive natural convection which could similarly reduce mixing times. However, in some cases where there is little movement, these sources of buoyancy could cause the air in the room to stratify so reducing large scale mixing. Mixing in spaces with natural ventilation is considered in detail by Coffey and Hunt [29] and Hunt and Kaye [30]. The automated method developed here could be extended to include more of these features if required.

The applicability of an automated CFD modelling tool has been demonstrated by studying mixing in mechanically ventilated indoor spaces. It would be possible to apply the tool to a range of indoor dispersion related problems. Using a HPC system, studies consisting of many independent simulations within a design space, can be run rapidly.

5. Conclusions

The time between the pollutant first reaching the occupied zone and most of the zone reaching a threshold concentration (where the threshold is a function of the well-mixed peak concentration) was demonstrated to be well represented by the relationship $t_{95\text{-}5} = 0.121\ \tau$. This relationship showed little dependence on the release duration when this was increased from 1 s to 100 s. The time did, however, reduce when the ratio of the well-mixed room peak concentration to the threshold concentration was increased from 10 to 100.

The results of the study show that in a room with an air change rate of 5 h^{-1} there would be approximately 1.5 min between a few people being exposed to the threshold concentration and the majority of the people in a room being exposed to the threshold concentration.

It has been demonstrated that the Drescher et al. [2] mixing model based on mechanical power can broadly be used to predict the time taken to reach a normalised standard deviation threshold in a mechanically ventilated room with ceiling mounted supply and extract and with the mixed pollutant being delivered via the supply vents.

A useful tool has been developed for studying indoor dispersion effects in a more generic sense than was previously achievable. Using this tool it is possible to create, solve and post process many hundreds of CFD models in a matter of days making it suitable for fast turnaround safety/resilience planning.

The generic results produced could then be used to inform a rapid emergency response. The CFD method used was successfully validated although it would be beneficial to extend the validation to include multiple data sets spanning the range of conditions used in the automated study.

Acknowledgements

The research was supported by the UK Ministry of Defence.

Appendix A. Supplementary data

Supplementary data related to this article can be found at http://dx.doi.org/10.1016/j.buildenv.2017.01.011.

References

[1] M.R. Sippola, W.W. Nazaroff, Modeling particle loss in ventilation ducts, Atmos. Environ. 37 (39–40) (2003) 5597–5609.
[2] A.C. Drescher, C. Lobascio, A.J. Gadgil, W.W. Nazaroff, Mixing of a point-source indoor pollutant by forced convection, Indoor Air 5 (1995) 204–214.
[3] A.V. Baughman, A.J. Gadgil, W.W. Nazaroff, Mixing of a point source pollutant by natural convection flow within a room, Indoor Air 4 (1994) 114–122.
[4] E. Lim, K. Ito, M. Sandberg, New ventilation index for evaluating imperfect mixing conditions–Analysis of Net Escape Velocity based on RANS approach, Build. Environ. 61 (2013) 45–56.
[5] G. Cao, H. Awbi, R. Yao, Y. Fan, K. Sirén, R. Kosonen, J.J. Zhang, A review of the performance of different ventilation and airflow distribution systems in buildings, Build. Environ. 73 (2014) 171–186.
[6] E. Mundt, H.M. Mathisen, P.V. Nielsen, A. Moser, Ventilation Effectiveness, REHVA, Brussels, Belgium, 2004.
[7] C.-A. Roulet, Ventilation and Airflow in Buildings: Methods for Diagnosis and Evaluation, Earthscan, London, UK, 2008.
[8] Q. Chen, Ventilation performance prediction for buildings: a method overview and recent applications, Build. Environ. 44 (2009) 848–858.
[9] K.-C. Cheng, V. Acevedo-Bolton, R.-T. Jiang, N.E. Klepeis, W.R. Ott, O.B. Fringer, L.M. Hildemann, Modeling exposure close to air pollution sources in naturally ventilated residences: association of turbulent diffusion coefficient with air change rate, Environ. Sci. Technol. 45 (2011) 4016–4022.
[10] G. Cao, M. Ruponen, R. Paavilainen, J. Kurnitski, Modelling and simulation of the near-wall velocity of a turbulent ceiling attached plane jet after its impingement with the corner, Build. Environ. 46 (2011) 489–500.
[11] H. Awbi, Ventilation of Buildings, Spon Press, New York, 2003.
[12] ASHRAE, ASHRAE Handbook of Fundamentals (2009), ASHRAE, Atlanta, GA, 2009.
[13] S. Corrsin, Simple theory of an idealized turbulent mixer, AICHE J. 3 (1957) 329–330.
[14] Y. Li, P.V. Nielsen, Commemorating 20 years of indoor air: CFD and ventilation research, Indoor Air 21 (2011) 442–453.
[15] A.J. Gadgil, C. Lobscheid, M.O. Abadie, E.U. Finlayson, Indoor pollutant mixing time in an isothermal closed room: an investigation using CFD, Atmos. Environ. 37 (2003) 5577–5586.
[16] I.M. Sobol, Distribution of points in a cube and approximate evaluation of integrals, U.S.S.R Comput. Maths. Math. Phys. 7 (1967) 86–112.
[17] R.B. Gramacy, H.K.K. Lee, Bayesian treed Gaussian process models with an application to computer modelling, J. Am. Stat. Assoc. 103 (483) (2008) 1119–1130.
[18] Icon, IconCFD Release 3.1 Technical User Guide, Icon, 2014.
[19] Trox Quick Reference Guide, 2013. http://www.troxuk.co.uk/uk/service/download_centre/structure/technical_documents/diffusers/quick_selection_guide.pdf. Last accessed: 28-05-2014.
[20] F. Porges, HVAC Engineer's Handbook, Butterworth-Heinemann, Oxford, UK, 2001.
[21] J. Gao, L. Zeng, L. Wu, X. Ding, X. Zhang, Solution for sudden contamination transport through air duct system: under a puff release, Build. Environ. 100 (2016) 19–27.
[22] C.B. Keil, C.E. Simmons, T.R. Anthony, Mathematical Models for Estimating Occupational Exposure to Chemicals, AIHA, Fairfax, VA, 2009.
[23] ARID, UVIC® MkII User's Manual, ARID Ltd, 2004.
[24] H. Wang, A. Zhai, Application of coarse-grid computational fluid dynamics on indoor environment modelling: optimizing the trade-off between grid resolution and simulation accuracy, HVAC&R Res. 18 (5) (2012) 915–933.
[25] D.N. Sorensen, P.V. Nielsen, Quality control in computational fluid dynamics in indoor environments, Indoor Air 13 (2003) 2–17.
[26] Y. Tominaga, T. Stathopoulos, Turbulent Schmidt numbers for CFD analysis with various types of flowfield, Atmos. Environ. 41 (2007) 8091–8099.
[27] J.Z. Zhai, Z. Zhang, W. Zhang, Q. Chen, Evaluation of various turbulence models in predicting airflow and turbulence in enclosed environments by CFD: part-1: summary of prevalent turbulence models, HVAC&R Res. 13 (6) (2007) 853–870.
[28] P.J. Drivas, P.A. Valberg, B.L. Murphy, R. Wilson, Modeling indoor air exposure from short-term point source releases, Indoor Air 6 (1996) 271–277.
[29] C.J. Coffey, G.R. Hunt, Ventilation effectiveness measures based on heat removal: Part 1. Definitions, Build. Environ. 42 (6) (2007) 2241–2248.
[30] G.R. Hunt, N.B. Kaye, Pollutant flushing with natural displacement ventilation, Build. Environ. 41 (9) (2006) 1190–1197.